Original Article

Analysis of the Electrophoretic Profiles of Prion Protein in Carcinous and Pericarcinous Lysates of Six Different Types of Cancers*

WEI Wei[1], WU Yue Zhang[2], XIAO Kang[2], XU Guo Hui[1], SONG Yun Tao[1], SHI Qi[2,#], and DONG Xiao Ping[2,3,4,5,#]

1. Key Laboratory of Carcinogenesis and Translational Research (Ministry of Education), Head and Neck Surgery Department, Peking University Cancer Hospital & Institute, Beijing 100142, China; 2. State Key Laboratory for Infectious Disease Prevention and Control, Collaborative Innovation Center for Diagnosis and Treatment of Infectious Diseases (Zhejiang University), National Institute for Viral Disease Control and Prevention, Chinese Center for Disease Control and Prevention, Beijing 102206, China; 3. Center for Global Public Health, Chinese Center for Disease Control and Prevention, Beijing 102206, China; 4. Wuhan Institute of Virology, Chinese Academy of Science, Wuhan 430071, Hubei China; 5. China Academy of Chinese Medical Sciences, Beijing 100700, China

Abstract

Objective To find the different electrophoretic profiles of prion protein in carcinous and individual pericarcinous tissues in lysates of gastric, colon, liver, lung, thyroid, and laryngeal cancers.

Methods Sodium dodecyl sulfate polyacrylamide gel electrophoresis (SDS-PAGE) and Western blot were used to test the amounts and electrophoretic patterns of total PrP and the tolerance of PK (protease K) digestion among six various cancer tissue types.

Results A mass of PrP signals with a large molecular weight were identified in the homogenates of peripheral tissues. The amounts and electrophoretic patterns of total PrP did not differ significantly between carcinous and pericarcinous tissues. PrPs in all types of the tested cancer samples were PK sensitive but showed diversity in the tolerance of PK digestion among various tissue types.

Conclusions The study revealed that the included electrophoretic patterns of carcinous and pericarcinous tissues were almost similar. Unlike PrP-specific immunohistochemical assay, evaluation of PrP electrophoretic patterns in the peripheral organs and tissues by Western blot does not reflect tumor malignancy.

Key words: Prion protein; Cancer; Electrophoretic profiles

Biomed Environ Sci, 2021; 34(9): 683-692 *doi: 10.3967/bes2021.096* *ISSN: 0895-3988*

www.besjournal.com (full text) *CN: 11-2816/Q*

INTRODUCTION

Prion protein (PrP) is a cellular membrane protein that is distributed in many kinds of tissue cells. PrP is attractive due to its conformational changed isoform PrP^{Sc}, which is the etiological agent for prion disease or transmissible spongiform encephalopathy. In this theory, the normal and physiological form of PrP (PrP^{C}) converts to abnormal and pathological isoform, leading to a pathogenesis of a special neurodegenerative disease with a short clinical course and 100% fatality rate[1]. As a conservative cellular protein, many functions have been proposed, such as cell signal transduction,

*This work was supported by the National Natural Science Foundation of China [grant no. 81630062] and the State Key Laboratory for Infectious Disease Prevention and Control [grant nos. 2019SKLID501, 2019SKLID603, and 2019SKLID307].

#Correspondence should be addressed to SHI Qi, Professor, PhD, Tel: 86-10-58900818, E-mail: shiqi76@126.com; DONG Xiao Ping, Professor, PhD, Tel: 86-10-58900815, E-mail: dongxp238@sina.com

Biographical note of the first author: WEI Wei, male, born in 1974, PhD Candidate, majoring in head and neck tumor.

cellular copper metabolism, cell adhesion, anti-apoptosis, migration, immune modulation, and cell differentiation[2]. However, depletion of PrP expression in knockout transgenic mice does not affect the development and function of the central nervous system and the life span[3]. PrP is a glycosylating protein, with two N-linked glycosylating sites at codon 181 Ser and 197 Ser at its C-terminus. According to the glycosylation on those sites, three main forms of PrP molecules can be seen, namely, di-, mono-, and aglycosylated PrPs, with about 5 kD difference in each glycosylation site[4]. In brain tissues, these three normal PrP^C bands migrate from 25 to 35 kD in sodium dodecyl sulfate polyacrylamide gel electrophoresis (SDS-PAGE). In the brains of prion diseases, e.g., human sporadic Creutzfeldt-Jakob disease (sCJD) and scrapie-infected experimental rodents, considerable amounts of PrP signals with large molecular weight are usually observable in Western blots, aside from the accumulation of a large amount of three forms of PrP monomers[5]. More importantly, the pathological PrP^{Sc} possesses partial proteinase K (PK) resistance, proteolyzing the N-terminal fragment and leading to the production of three truncated PrP bands ranging from 19 to 25 kD. Such characteristics are used to distinguish PrP^C and PrP^{Sc} in brain tissues of prion disease[6]. Differences of brain PrP in the ratios of glycosylating isoforms, electrophoretic patterns in SDS-PAGE, lengths of the degraded fragments, and tolerance to PK digestion are associated with different types of prion diseases, prion strains, and susceptibilities to prion infection.

Aside from its critical role in prion disease, the potential roles of cellular PrP in human malignant tumors have also been addressed. With the use of immunohistochemical techniques, PrP overexpression has been identified in a variety of malignant tumors, including laryngeal, gastric, pancreatic and breast carcinomas, osteosarcoma, and melanoma[7]. PrP overexpression is proposed to be closely associated with poor prognosis of pancreatic and breast cancers, highlighting that PrP may affect the growth and invasiveness of cancers. A study also demonstrated the important role of PrP overexpression in the acquisition of multidrug-resistant gastric cancer[8]. However, the profiles of PrP in malignant tumors, such as the electrophoretic patterns of SDS-PAGE and the features of PK resistance, have not been addressed extensively.

To determine the profiles of PrP molecules in malignant tumors, we collected different numbers of surgically removed samples of gastric, colon, liver, lung, thyroid, and laryngeal cancers, as well as individual pericarcinous tissues. After tissue homogenates were prepared, the electrophoresis patterns of PrP proteins were analyzed by PrP-specific Western blot. We found that the electrophoretic patterns of carcinous and pericarcinous tissues were similar but markedly different from those of brain tissues. The amounts of total PrP evaluated by western blot did not differ significantly between carcinous and pericarcinous tissues. PrPs in all types of the tested cancers were PK sensitive, but showed diversity in the tolerance of PK digestion among various tissue types.

MATERIALS AND METHODS

Specimens

All cancer specimens were collected from Peking University Cancer Hospital and Institute with pathological diagnosis. Cancer and pericarcinous tissues were removed surgically and frozen at −80 °C for further usage. The specimens tested in this study included 10 gastric cancers (adenocarcinoma), 5 colon cancers (adenocarcinoma), 5 liver cancers (hepatocellular carcinoma), 9 lung cancers (squamous cell carcinoma), 10 thyroid cancers (papillary carcinoma), and 10 laryngeal cancers (squamous cell carcinoma). All samples enrolled in this study were pathologically confirmed by the pathologists in Peking University Cancer Hospital and Institute, with the TNM staging method identifying advanced clinical stages, namely, two lung cancers at stage IV and the rest at stage III. The study was approved by the Ethical Committee of Peking University Cancer Hospital and Institute.

Preparations of Tissue Homogenates

Tissue samples from various carcinomas and the pericarcinous tissues, as well as tissues from human and hamster brains, were washed in Tris-buffered saline (TBS, 10 mmol/L Tris-HCl, 133 mmol/L NaCl, pH 7.4) at least three times. Each sample was mixed in the lysis buffer (100 mmol/L NaCl, 10 mmol/L EDTA, 0.5% NP-40, 0.5% sodium deoxycholate, 10 mmol/L Tris, pH 7.4) containing protease inhibitor cocktail set III at the ratio of 1:10 (w/v) and then homogenized mechanically. The preparations were centrifuged at 2,000 ×*g* for 10 min or 20,000 ×*g* for 30 min to discard the tissue debris, and the supernatant fractions were collected separately and stored at −80 °C for further experiments.

Western Blots

Aliquots of tissue homogenates were separated in 12% SDS-PAGE and electroblotted onto nylon membranes with a semi-dry facility. Membranes were blocked in TBS containing 5% skimmed milk at room temperature (RT) for 2 h and incubated with various primary antibodies at 4 °C overnight, including PrP-specific monoclonal antibodies 3F4 (MAB1562), 4H7 (Santa-58579), 6D11 (Santa-58581), 7D9 (Santa-58582), 8H4 (Abcam 61409) and SAF32 (SPI-Bio A03202), and anti-β-actin antibody (1:5,000, Zhongshanjinqiao, tg09). After being washed with TBS containing 0.1% Tween 20, the membranes were incubated with HRP-conjugated secondary antibodies (Jackson ImmunoResearch Labs, 115-035-003 and 111-035-003) at RT for 1 h. The blots were developed using an enhanced chemiluminescence system (ECL, PerkinElmer, NEL103E001EA) and visualized on autoradiography films (General Electrics).

Proteinase K (PK) Digestion

To evaluate the PK resistances of PrP proteins in cancer tissues, 10% tissue homogenates were exposed to different concentrations of PK, including 20, 50, 100, 250, 500, and 1,000 μg/mL. The digestion was performed at 37 °C for 1 h and stopped by boiling in a loading buffer. The preparations were immediately subjected to 12% SDS-PAGE and Western blots with mAb 3F4. For positive control of PrP^{Sc}, 10% brain homogenates (BHs) of human sCJD or 263K-infected hamster were incubated with a final concentration of 20 μg/mL proteinase K at 37 °C for 1 h prior to western blots.

PrP Deglycosylation

A total of 15 μL aliquot of tissue homogenates were boiled for 10 min in denaturing buffer (0.5% SDS, 1% β-mercaptoethanol) and deglycosylated with 1,500 U PNGase F (Biolab) in 1% Nonidet P-40, 50 mol/L sodium phosphate, pH 7.5 at 37 °C for 12 h. Proteins were precipitated with 4 volumes of cold methanol at −20 °C for 6 h and centrifuged at 15,000 ×*g* for 30 min. The pellets were resuspended and separated in 12% SDS-PAGE and PrP-specific Western blots with mAb 3F4.

Statistical Assays

The Western blot images were captured by ChemiDoc ™ XRS + Imager and quantified by ImageJ software. Statistical analyses were performed using Student's *t*-test. All data were presented as mean + SEM.

RESULTS

The PrPs in the Tissues of the Malignant Tumors Show Different Electrophoretic Patterns in Western Blots Compared with that of Brain Tissues

To observe the presence and the electrophoretic profiles of the PrP proteins in the malignant tissues, three randomly selected prepared tissue homogenates of each type of cancer were pooled and subjected to Western blots with PrP mAb 3F4. In parallel, the BH from an sCJD case, a normal donor that died of a car accident, and scrapie agent 263K-infected hamster were loaded as the control. Three PrP-specific bands were clearly observed in the preparations of brain specimens, which were at the positions from 25 to 35 kD, representing di-, mono-, and non-glycosylated PrPs (Figure 1). Larger molecular weights of PrP-specific signals were also detected in the BH of sCJD and 263-infected hamsters. In contrast, the pooled samples of cancer tissues displayed distinguishing electrophoretic patterns, containing more positive blotted bands (Figure 1). The most predominant bands were larger molecular weight signals, which migrated at almost the same position as those in the BH. Clear positive bands at the position of monoglycosylated PrP were detected in all tumor preparations, while the bands at the position of aglycosylated bands corresponding to diglycosylated PrP were relatively weak (Figure 1). In addition, the PrP reactive patterns in Western blots of all tested cancers seemed to be similar, and the amounts of PrP positive signals were indistinguishable in the digital assays of the relative gray values of PrP signals normalized with the individual β-actin (Figure 1).

To further assess the glycosylating features of PrP signals in tumor tissues, the homogenates of three laryngeal carcinomas and two benign polys underwent deglycosylation together with or without PK digestion. In the reaction of PNGase F without PK treatment (Figure 2A, middle panel), all tested laryngeal samples exhibited distinct PrP signals at the approximate position of 25 kD, which migrated at the same position as the PrP signals in the brain samples of healthy or diseased human and hamster. A weak and small molecular signal was also observed in some malignant tissues, which was slightly higher in SDS-PAGE than in brain tissues. In the preparation of PNGase F after 20 μg/mL PK digestion (Figure 2A, bottom panel), as expected, the PrP signals in the

normal human and hamster brain samples disappeared, whereas those in the sCJD case and 263K-infected hamster shifted to a position slightly higher than 20 kD. PrP-specific signals were still detectable in the three tested malignant cancers and seemed to be still slightly higher than those in the brain samples of prion diseases. No or a very faint PK-resistant PrP signal was observed in the homogenates of two benign laryngeal polys.

Subsequently, the immunoreactivities of PrP signals in tumor tissues were tested by Western blots with various PrP-specific mAbs. The pooled samples from three gastric cancers and the pooled samples of the pericarcinous tissues from the same three cases were subjected to the tests, with the brains of 263K-infected hamsters used as the control. As shown in Figure 2B, two predominate PrP bands were observed in all reactions; one had a large molecular weight signal and the other was at the position of monoglycosylated PrP. In addition to the difference in signal strength, the reactive profiles to various PrP antibodies appeared similar. The PrP reactive profiles in carcinous and pericarcinous tissues were also comparable, thereby indicating that the PrPs in the cancer tissues are probably full-length ones.

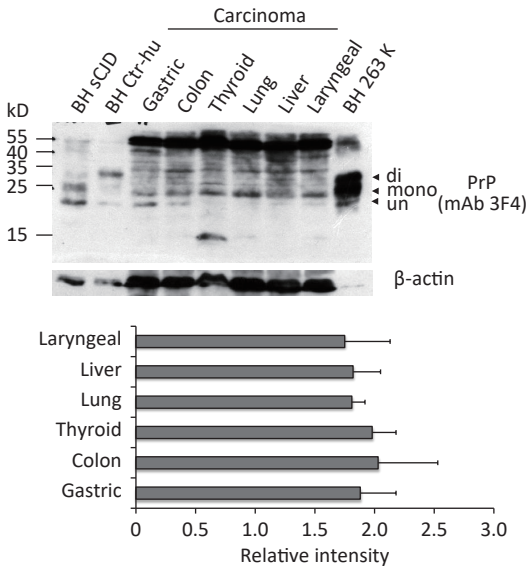

Figure 1. Representative PrP-specific Western blot of the pooled homogenates of six different cancer tissues (upper panel). Randomly selected lysates of three individual tissues of each kind of carcinoma were mixed as the pooled homogenate. BH of a normal person who died of a car accident, an sCJD patient, and a scrapie agent 263K-infected hamster were used as controls. All preparations underwent Western blot with PrP mAb 3F4 without PK digestion. Di: diglycosylated; Mono: monoglycosylated; Un: unglycosylated. The densities of signals were determined by densitometry of all PrP signals and shown as relative intensity after being normalized with the individual values of β-actin. Graphical data denote mean + SD (bottom panel).

No Significant Difference in PrP Amount between Carcinous and Pericarcinous Tissues is Observed by Western Blots

The abnormal changes of PrP in various kinds of human malignant tissues are widely described, mostly based on immunohistochemical assays[9]. To evaluate the potential PrP diversity in electrophoretic patterns, different numbers of carcinous tissues from gastric, colon, liver, lung, thyroid, and laryngeal cancers were collected and used in Western blots with mAb 3F4 together with the individual pericarcinous tissues in parallel. In general, the PrP reactive patterns were similar between carcinous and pericarcinous tissues (Figure 3). Quantitative assays of the average gray values of total PrP signals after normalization with the individual actin showed slightly higher values in the carcinous tissues of gastric (Figure 3A), liver (C), thyroid (E), and laryngeal (F) cancers, and in the pericarcinous tissues of the colon (B) and lung (D), without statistical significance. This finding highlights that under our experimental condition, either PrP reactive profiles or intensities in the carcinous and pericarcinous tissues are undistinguishable by the Western blots.

The PrPs in the Carcinous and Pericarcinous Tissues are PK Sensitive, but Vary among the Tissue Types

To test the features of PK resistance of PrPs in various tumors, the pooled carcinous and pericarcinous samples consisting of randomly selected three cases were prepared. After exposure to different concentrations of PK for 1 h, the digestions were stopped and subjected to Western blots immediately. As shown in Figure 4, the PrP signals in all tested tissue kinds of carcinous and pericarcinous samples were reduced in a dose-dependent manner. PrPs in all types of the tissues were partially but clearly PK resistant to the digestion of 20 μg/mL. At the same PK working concentration (20 μg/mL), the PrP signal in the normal BH vanished completely (data not shown).

Along with the increase in the PK amount, the PrP signals with a large molecular weight completely disappeared, whereas those with a small molecular weight were remarkably weaker and eventually undetectable. Different tissue types seemed to show slight diversity of PK resistances. Quantitative measures of the average gray values revealed that compared with data without PK, PrP signals in gastric (Figure 4A) and colon (D) tissues reduced to 20%–60% in the reaction of 20 μg/mL and less than 7% in the reaction of 50 μg/mL. The PrP signals in the tissues of the liver (C), lung (D), and thyroid (E) seemed to be more sensitive to PK digestion, which reduced to be almost undetectable in the

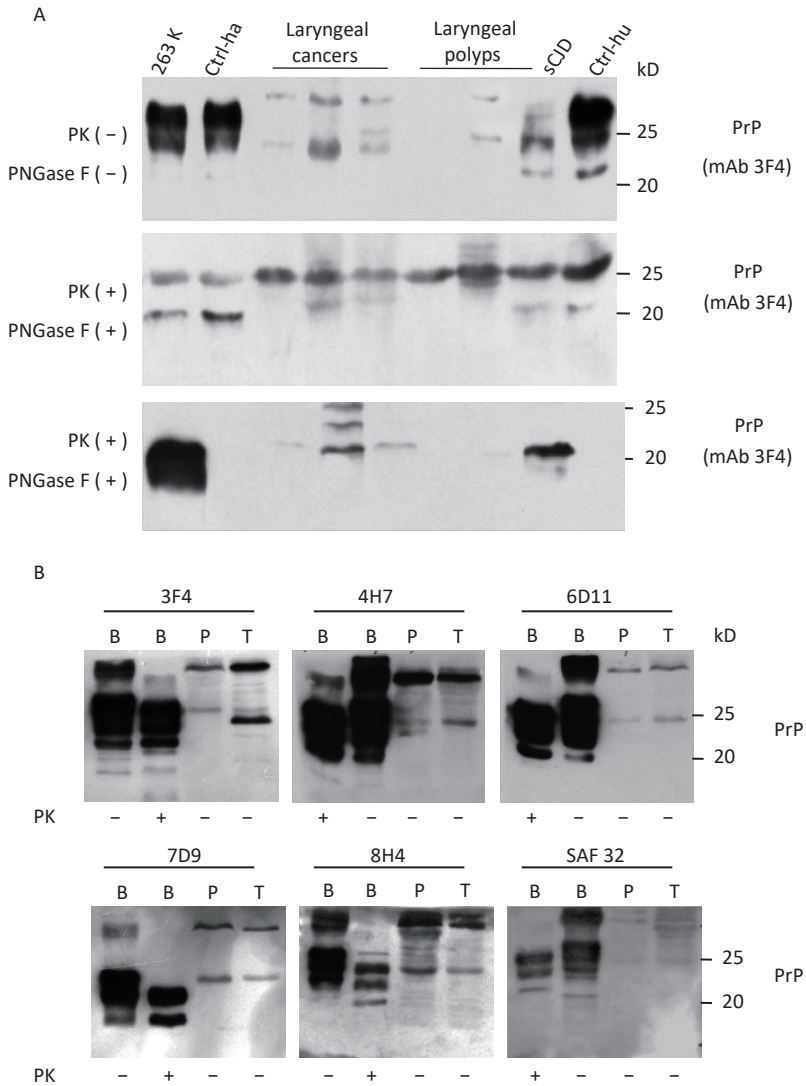

Figure 2. Evaluation of the glycosylating and immunoreactive features of PrPs in the carcinous tissues. (A) Diglycosylation with PNGase F. The homogenates of three laryngeal carcinomas and two benign polys were included, together with the brain lysates of normal and 263K-infected hamsters, as well as those of normal donor and sCJD patients as controls. Upper panel: The lysates without treatment of PNGase and PK. Middle panel: The lysates treated with PNGase, but without PK. Lower panel: The lysates treated with PNGase and PK (20 μg/mL). (B) Immunoreactivities with various PrP-specific mAbs. The pooled homogenates of gastric carcinous (T) and pericarcinous tissues (P) were subjected to Western blot with PrP-specific mAbs 3F4, 4H7, 6D11, 7D9, 8H4, and SAF32, respectively. BH: brain homogenates. The BH of 236K-infected hamsters treated with PK (20 μg/mL) and without PK were loaded as controls. The loading volume for tumor homogenate is 20 μL, and the volume for BH is 15 μL.

preparation of 50 μg/mL PK. The PrP signals in laryngeal tissues (F) were markedly more PK resistant, which maintained 70% signals in the reaction of 20 μg/mL and about 25% in that of 50 μg/mL PK. A comparison of the PK resistance of PrP signals in carcinous and pericarcinous tissues suggests that the PrP signals in malignant tissues tend to have a slightly stronger tolerance to PK digestion. These data indicate that the PrPs in the malignant tumors are generally PK sensitive.

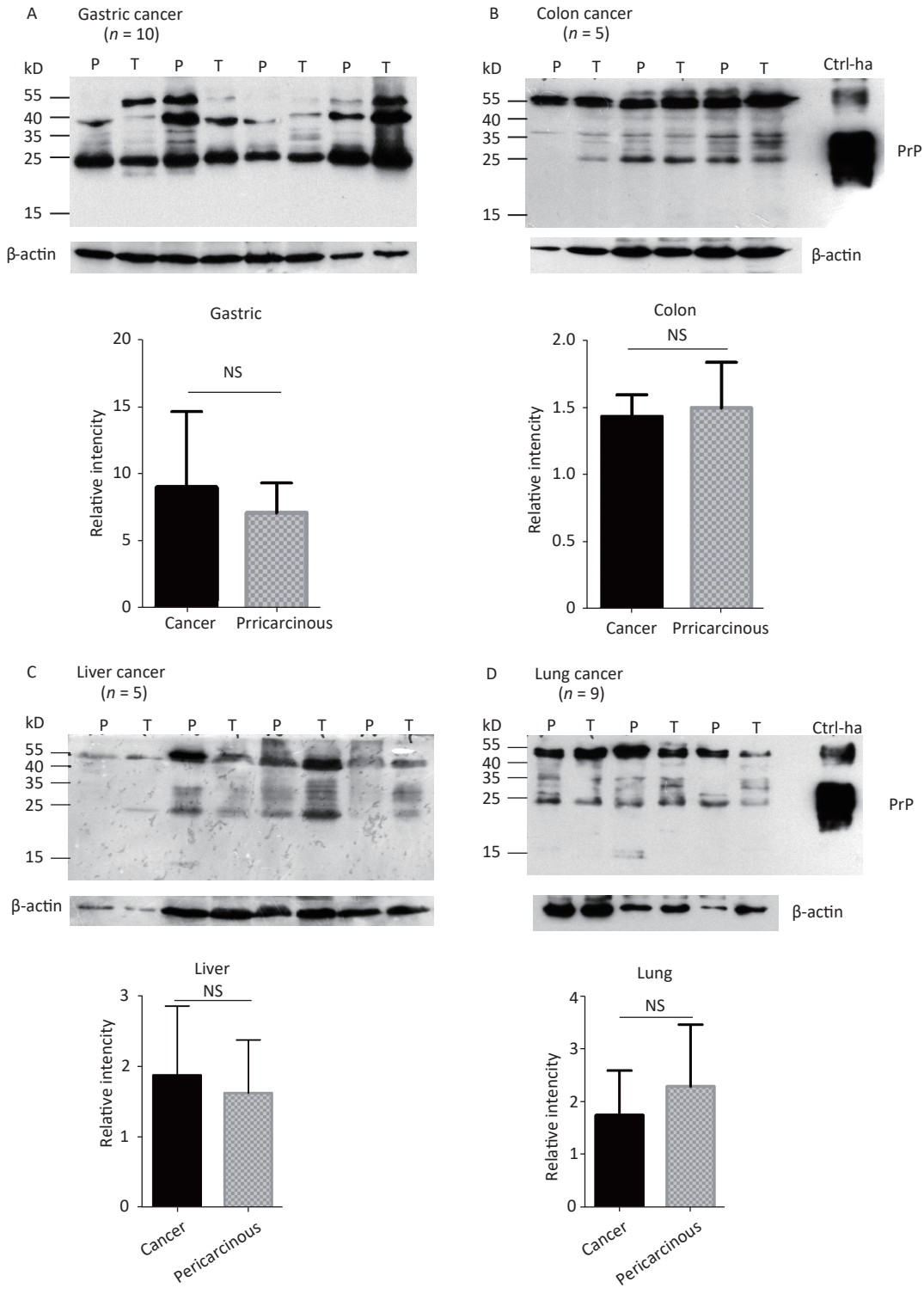

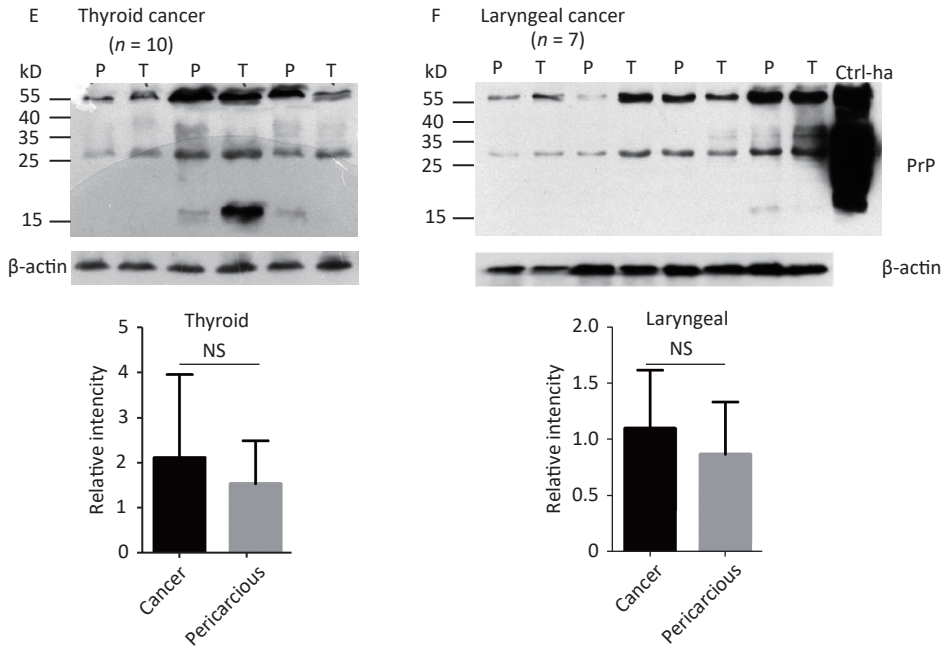

Figure 3. Representative Western blots of the PrPs in the homogenates of paired carcinous and pericarcinous tissues. (A) Gastric cancer (*n* = 10). (B) Colon cancer (*n* = 5). (C) Liver cancer (*n* = 5). (D) Lung cancer (*n* = 9). (E) Thyroid cancer (*n* = 10). (F) Laryngeal cancer (*n* = 7). The antibody used in Western blots was mAb 3F4. The densities of signals are determined by densitometry of all PrP signals and shown as relative intensity after being normalized with the individual values of β-actin. Graphical data denote mean + SD and are shown at the bottom of each representative graph.

DISCUSSION

In this study, we screened the electrophoretic and immunoreactive patterns of PrPs in six types of human malignant tumors and their pericarcinous tissues. All tested samples, whether carcinous or pericarcinous tissues, contain similar PrP electrophoretic patterns that are distinctly different from that of brain tissues, regardless of whether the condition is normal or prion disease. We also tested the PrP electrophoretic patterns in different tissue homogenates from normal mice, including the heart, liver, spleen, and lung. As indicated in Supplementary Figure S1 (available in www.besjournal.com), similar PrP electrophoretic profiles are observed, showing predominate amounts of large molecular weight PrP signals. We prepared the tissue homogenates at different centrifuging speeds (2,000 and 20,000 rpm) to exclude the possible influence of tissue debris in SDS-PAGE. Little change in the PrP patterns was observed, aside from a slight increase in the amounts of PrP monomers in some tissues, e.g., heart and lung (Supplementary Figure S1). The PrP electrophoretic patterns do not seem to be associated with malignancy but rather reflect the feather of PrP in the peripheral tissues.

We found large quantities of PrP signals with a large molecular weight in the homogenates of peripheral tissues, with the bands roughly at the 55 kD position being predominate. Such large molecular weight PrP signals can also be observed in the homogenates of brain tissues, especially in the brains of prion diseases, but showing apparently lower amounts compared with the PrP monomers[10]. Although we do not have the direct data of amino acid (aa) sequence for such bands, on the basis of the molecular weight and the immunoreactivity to PrP antibodies, such bands might be the dimer of PrP molecules. PrP dimer is observable in normal brain tissues, in some cultured mammalian cells, and even in the prokaryotic lysates expressing recombinant PrP[11]. As the smallest aggregate, PrP dimer can be disulfide bonded or non-disulfide linked[12]. On the basis of the recombinant human PrP proteins, they even illustrate that three motifs with PrP peptide modulate PrP dimerization, the negative motif of residues 36–42, and positive ones of residues 90–125 and residues 195–212[13]. Our data indicate that the majority of PrP molecules in the lysates of peripheral tissues seem to be full-length PrP, as

indicated by the wide reactivities with various PrP mAbs of different recognizing sites, such as mAbs SAF32 and 6D11 in the N-terminus, mAbs 8H4, 4H7 and 7D9 in C-terminus, and mAb 3F4 in aa. 112–115.

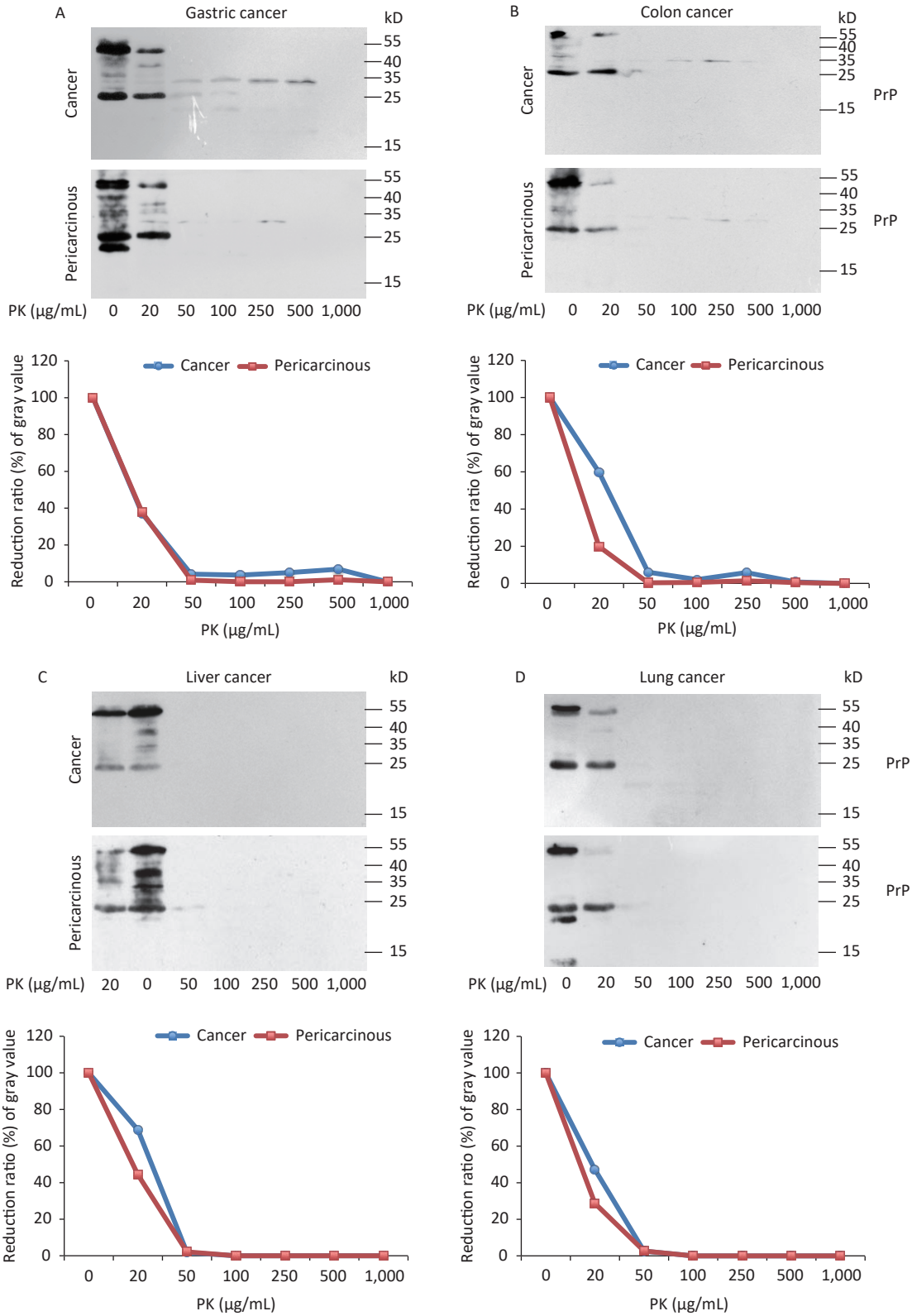

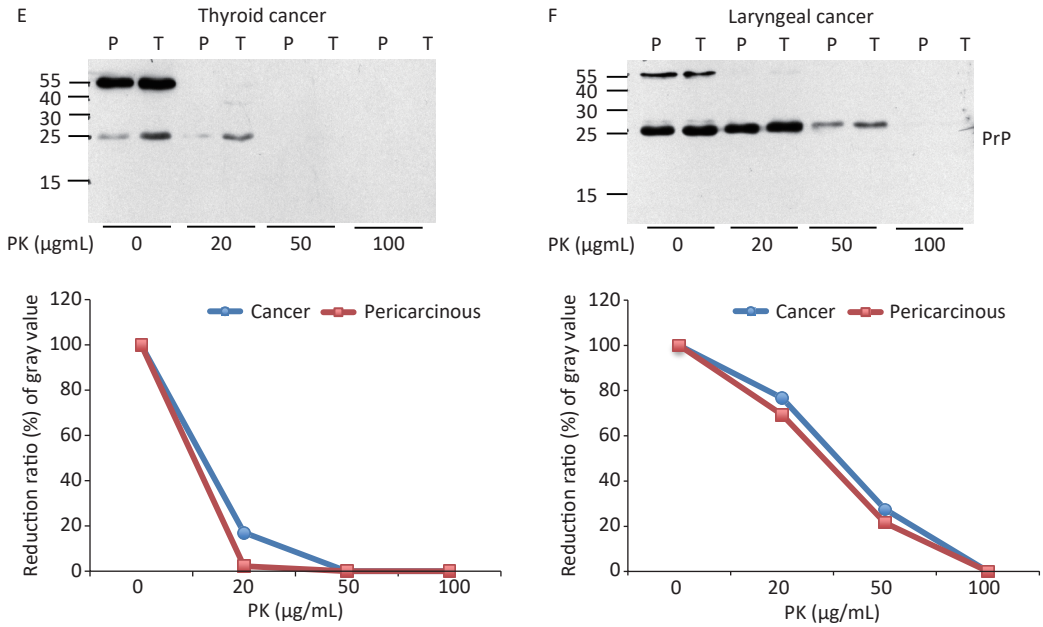

Figure 4. PK-resistant activities of the PrPs in the homogenates of paired carcinous and pericarcinous tissues. The pooled homogenates of six different cancer and pericarcinous tissues were exposed to different concentrations of PK prior to SDS-PAGE. (A) Gastric cancer. (B) Colon cancer. (C) Liver cancer. (D) Lung cancer. (E) Thyroid cancer. (F) Laryngeal cancer. The antibody used in Western blots was mAb 3F4. The densities of signals were determined by densitometry of all PrP signals and shown as relative intensity after being normalized with the individual values of β-actin. Graphical data of the individual tissue types are shown at the bottom of each representative graph.

More aggregative forms of PrP, which are represented by PrP dimers and oligomers, in the peripheral tissues than in brain tissues may suggest diverse PrP post-translational modifications.

Our PrP-specific western blots do not illustrate a significant difference either in the pattern or in the amount of PrPs between the carcinous and pericarcinous tissues. PrP overexpression in a number of malignant tumors has been documented repeatedly, but most of the studies are conducted with PrP-specific immunohistochemistry (IHC) assays[14-16]. The exact reason for such diversity using different techniques is known. One possibility is that the PrP antibodies only recognize linear epitopes in western blot, whereas they react with both linear and conformational epitopes in IHC. The stronger PrP signals of carcinous slices in IHC tests might derive from the reactions of PrP conformational epitopes with PrP-specific antibodies. Whether the transcription of the PrP encoding gene changed is unclear and needs further study.

We found that the PrPs in the peripheral tissues show weak PK resistance that is slightly but obviously stronger than that of the PrPs in brain tissues. These PK resistances of the PrPs from different tissue lysates also look slightly different. PrPs in laryngeal tissues are more PK resistant, followed by the PrP in the stomach and colon, while PrPs from liver, lung, and thyroid tissues are less PK resistant. Normal PrP proteins show PK resistance during aggregation. The PrP proteins with disease-associated mutations are more prone to forming aggregates and to displaying PK resistance *in vitro*[17]. Unlike the PrP^{Sc} in prion diseases, those aggregated PrPs certainly do not have infectivity[18]. More importantly, the PK-digested products of the aggregated normal and mutated PrPs usually do not shift down during electrophoresis[19,20], which means the conformational structures of the aggregated PrPs are different from those of PrP^{Sc}. We may assume that the weak PK resistances of PrPs in peripheral tissues are likely due to more PrP dimers and polymers.

AUTHOR CONTRIBUTIONS

SHI Qi and DONG Xiao Ping designed this work. WEI Wei collected the cancer samples, participated in the diagnosis, and analyzed the data. WU Yue Zhang and XIAO Kang performed the experiments.

XU Guo Hui and SONG Yun Tao performed the statistical analysis.

CONFLICTS OF INTEREST

The authors declare no competing financial interest.

Received: November 24, 2020;
Accepted: May 19, 2021

REFERENCES

1. Asher DM, Gregori L. Human transmissible spongiform encephalopathies: historic view. Handb Clin Neurol, 2018; 153, 1−17.
2. Watts JC, Bourkas MEC, Arshad H. The function of the cellular prion protein in health and disease. Acta Neuropathol, 2018; 135, 159−78.
3. Weissmann C, Flechsig E. PrP knock-out and PrP transgenic mice in prion research. Br Med Bull, 2003; 66, 43−60.
4. Fiorini M, Bongianni M, Monaco S, et al. Biochemical characterization of prions. Prog Mol Biol Transl Sci, 2017; 150, 389−407.
5. Castle AR, Gill AC. Physiological functions of the cellular prion protein. Front Mol Biosci, 2017; 4, 19.
6. Lehmann S. The prion protein. J Soc Biol, 2002; 196, 309−12.
7. Yang XW, Zhang Y, Zhang LH, et al. Prion protein and cancers. Acta Biochim Biophys Sin, 2014; 46, 431−40.
8. Hinton C, Antony H, Hashimi SM, et al. Significance of prion and prion-like proteins in cancer development, progression and multi-drug resistance. Curr Cancer Drug Targets, 2013; 13, 895−904.
9. Liang J, Bai FH, Luo GH, et al. Hypoxia induced overexpression of PrP^{C} in gastric cancer cell lines. Cancer Biol Ther, 2007; 6, 769−74.
10. MacLea KS. What makes a prion: infectious proteins from animals to yeast. Int Rev Cell Mol Biol, 2017; 329, 227−76.
11. Colby DW, Prusiner SB. Prions. Cold Spring Harb Perspect Biol, 2011; 3, a006833.
12. Taguchi Y, Lu L, Marrero-Winkens C, et al. Disulfide-crosslink scanning reveals prion-induced conformational changes and prion strain-specific structures of the pathological prion protein PrP^{Sc}. J Biol Chem, 2018; 293, 12730−40.
13. Gao ZX, Shi J, Cai LL, et al. Prion dimer is heterogenous and is modulated by multiple negative and positive motifs. Biochem Biophys Res Commun, 2019; 509, 570−6.
14. Wei W, Shi Q, Zhang NS, et al. Expression of prion protein is closely associated with pathological and clinical progression and abnormalities of p53 in head and neck squamous cell carcinomas. Oncol Rep, 2016; 35, 817−24.
15. Zhou L, Shang YL, Liu CH, et al. Overexpression of PrPc, combined with MGr1-Ag/37LRP, is predictive of poor prognosis in gastric cancer. Int J Cancer, 2014; 135, 2329−37.
16. Diarra-Mehrpour M, Arrabal S, Jalil A, et al. Prion protein prevents human breast carcinoma cell line from tumor necrosis factor α-induced cell death. Cancer Res, 2004; 64, 719−27.
17. Marrone A, Re N, Storchi L. The effects of Ca^{2+} concentration and E200K mutation on the aggregation propensity of PrP^{C}: a computational study. PLoS One, 2016; 11, e0168039.
18. Muramoto T. Prion protein structure and its relationships with pathogenesis. Rinsho Shinkeigaku, 2003; 43, 813−6.
19. Mishra R, Elgland M, Begum A, et al. Impact of N-glycosylation site variants during human PrP aggregation and fibril nucleation. Biochim Biophys Acta Proteins Proteom, 2019; 1867, 909−21.
20. Paciotti R, Storchi L, Marrone A. An insight of early PrP-E200K aggregation by combined molecular dynamics/fragment molecular orbital approaches. Proteins, 2019; 87, 51−61.